ACS OMEGA

http://pubs.acs.org/journal/acsodf

Article

Investigation of Petroleum Coke Gasification with CO_2/H_2O Mixtures and S/N Removal Mechanism via ReaxFF MD Simulation

Jiazhuang Tian, Qiuyun Mao,* Zihan You, and Qifan Zhong*

Cite This: *ACS Omega* 2023, 8, 18140−18150

Read Online

ACCESS | Metrics & More | Article Recommendations | Supporting Information

ABSTRACT: The removal of environmentally harmful S/N is crucial for utilization of high-S petroleum coke (petcoke) as fuels. Gasification of petcoke enables enhanced desulfurization and denitrification efficiency. Herein, petcoke gasification with the mixture of two effective gasifiers (CO_2 and H_2O) was simulated via reactive force field molecular dynamics (ReaxFF MD). The synergistic effect of the mixed agents on gas production was revealed by altering the CO_2/H_2O ratio. It was determined that the rise in H_2O content could boost gas yield and accelerate desulfurization. Gas productivity reached 65.6% when the CO_2/H_2O ratio was 3:7. During the gasification, pyrolysis occurred first to facilitate the decomposition of petcoke particles and S/N removal. Desulfurization with the CO_2/H_2O gas mixture could be expressed as thiophene-S → S → COS → CHOS, thiophene-S → S → HS → H_2S. The N-containing components experienced complicated mutual reactions before being transferred into CON, H_2N, HCN, and NO. Simulating the gasification process on a molecular level is helpful in capturing the detailed S/N conversion path and reaction mechanism.

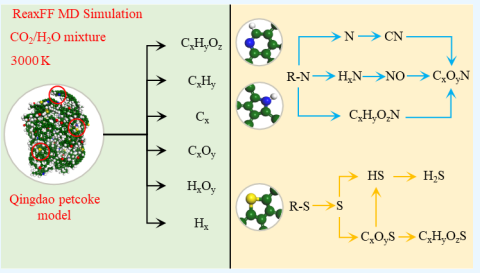

1. INTRODUCTION

Petroleum coke (petcoke) is a valuable oil refinery product derived from delayed coking of carbon−hydrogen compounds (such as petroleum asphalt and residual oil). As fuel, it is competitive because of the price advantage, extraordinary heat value (30.25−34.91 MJ/kg), high carbon (>80 wt %), and low ash (<1.5 wt %) content.[1−3] Nonetheless, due to the continuous decline in crude oil quality in recent years, petcoke high in S (>4 wt %) and N (∼1 wt %) content gradually dominates in the application of petcoke.[4−6] The extensive S and N elements in these petcoke are attributed to a large quantity of SO_x and NO_x emission and can aggravate environmental pollution.[7] As a result, the direct energy use of petcoke is doomed. Although efforts such as thermal desulfurization and alkali metal compound desulfurization have been made, technological and economic obstacles remain.[8−10] Therefore, a productive and environmentally benign technique must be adopted to facilitate the further practice of petcoke.

Gasification is an efficient and facile industrial technology for the transformation of carbonaceous materials into synthetic gas (syngas) by agents such as air, oxygen, and water. Its raw materials range broadly from coal to lignocellulosic wastes such as marc and pistachio exocarp.[11,12] During the process, S and N elements migrate to the gas phase as H_2S, NH_3, and HCN, among others, to reduce pollution.[13,14] This provides a promising methodology for the utilization of petcoke and the removal of the stubborn thiophene-S, pyrrole-N, and pyridine-N.[15] Rana et al.[16] employed supercritical water (SCW) in petcoke gasification due to its enhanced solubility and mass transfer properties. Under the effect of this single agent, H_2 yields multiplied by 74% as the SCW and the petcoke system was heated from 350 to 650 °C. Gasification agents including H_2, O_2, and NH_3 were also discussed in the corresponding research.[17−19] By mixing various gasification agents such as CO_2, O_2, H_2O, etc., enhanced syngas heat value, optimized gasifier utilization, and suppressed S- and N-containing gas emission can be achieved.[20−22] Kislov et al.[23] combined experiments with numerical simulation in the case of coal gasification by a mixture of air and CO_2. It was determined that the addition of CO_2 and H_2O into the air increased the caloric value of the gaseous product. Recently, Sharma et al.[24] investigated the Indian biomass gasification under an air-steam environment and achieved an enhanced H_2 productivity compared to that of air.

Microcrystalline structure, pore structure, and particle size have been considered to have a dramatic influence on petcoke gasification reactivity.[25,26] For example, Huo et al.[25] studied the correlation between the influencing factors of gasification reactivity. With a large particle size (∼250 μm) and high temperature (>1273 K), the petcoke gasification rate decreased due to the effect of pore diffusion. Zhou et al.[27] compared the gasification reactivity of petcoke and semicoke, a solid fuel

Received: March 3, 2023
Accepted: April 21, 2023
Published: May 10, 2023

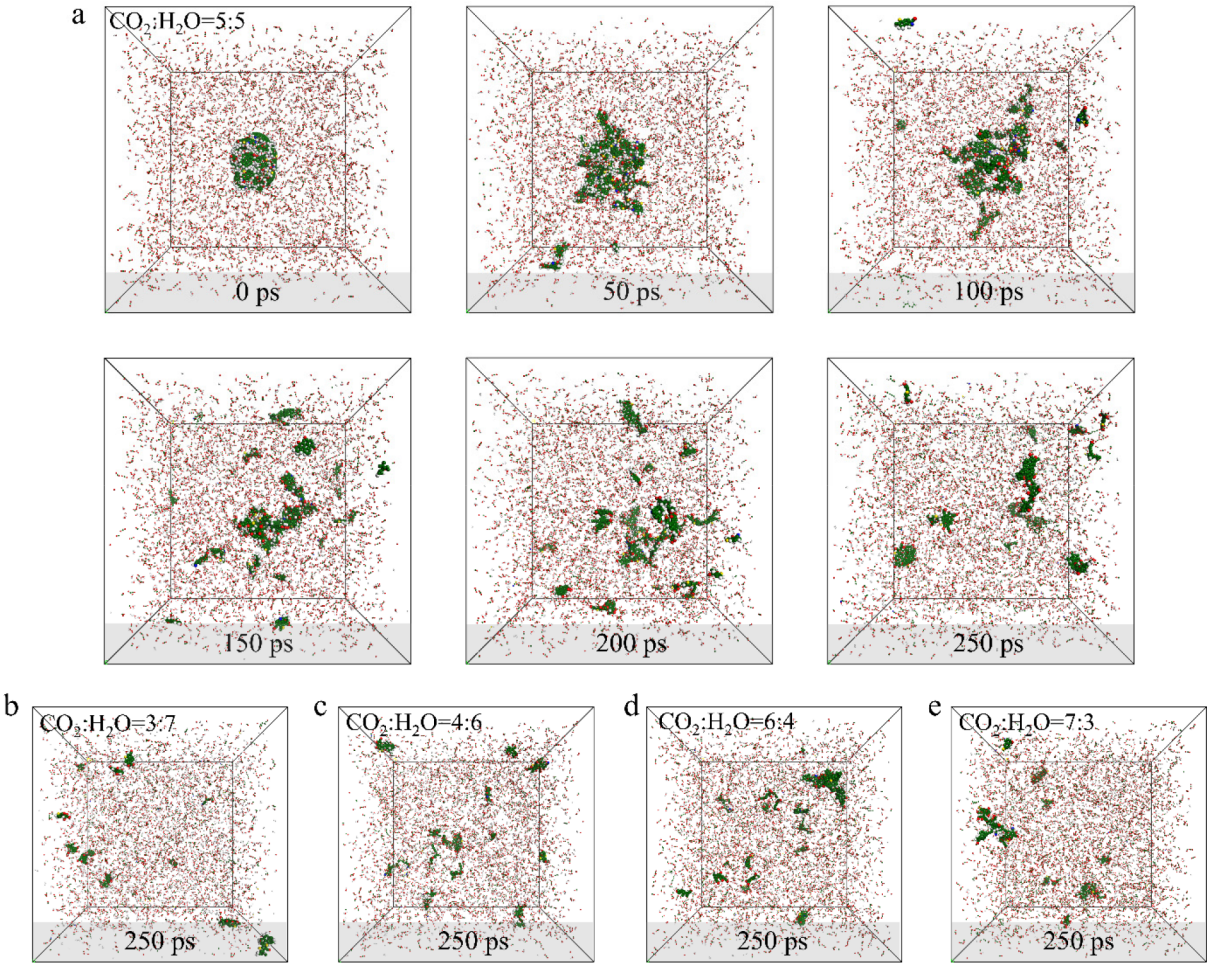

Figure 1. Snapshots of petcoke gasification process at different stage in ReaxFF MD simulation with CO_2/H_2O ratios of (a) 5:5, (b) 3:7, (c) 4:6, (d) 6:4, and (e) 7:3 (green for C atoms, white for H atoms, red for O atoms, yellow for S atoms, and blue for N atoms).

derived from heat treatment of petcoke. It was found that the low graphitization degree of semicoke resulted in a more disordered microcrystalline structure and thus exposed more active sites to facilitate the reaction. The transformation mechanism of the crucial intermediate products, such as OH and H radicals, is crucial to gasification characteristics. However, the lack of detection methods for such products hinders the further understanding for petcoke gasification.[26] To achieve a comprehensive understanding of the petcoke gasification mechanism and conversion path, research on a molecular level needs to be conducted.

A reactive force field molecular dynamics (ReaxFF MD) approach is capable of handling the mechanism study of intricate hydrocarbon systems such as petcoke. Castro-Marcano et al.[28] conducted a ReaxFF MD simulation for Illinois No. 6 coal char combustion research. The reaction system involved a 7458 atom char model and up to 14000 O_2 molecules. It was found that the 6-membered rings in char would be transferred into 5- and 7-membered rings. The decomposed small molecules would be oxidized by O and OH radicals. Bhoi et al.[29] constructed a ReaxFF MD system to explore the combustion and pyrolysis behaviors of brown coal. The system used was 100 times faster than quantum mechanics methods. Thus, as an atomic level calculation, large-scale (over 10000 atoms) ReaxFF MD simulation is practical in expense while retaining efficiency and accuracy.[30]

Herein, a Qingdao petcoke model from a previous study ($C_{1648}H_{772}O_{59}N_{24}S_{47}$) was used to conduct the ReaxFF MD simulation.[31,32] A mixture of CO_2/H_2O was introduced as the petcoke gasification agent. The productivity and component of the gaseous products were investigated. The existing forms of S/N elements and their transformation paths during gasification were investigated in the reaction mechanism study. The results of this work can help establish the connection between mechanism and productivity in petcoke gasification with a CO_2/H_2O mixture.

2. METHODS

2.1. Petcoke Model Introduction and Its Properties.

The gasification system involved a typical Qingdao high-S petcoke model ($C_{1648}H_{772}O_{59}N_{24}S_{47}$) and 4000 CO_2/H_2O molecules in total. In the previous work,[31,32] the petcoke model was well constructed and rationalized by X-ray photoelectron spectroscopy (XPS), Fourier transform infrared (FT-IR) spectroscopy, matrix-assisted laser desorption/ionization time-of-flight mass spectrometry (MALDI-TOF MS), X-ray powder diffraction (XRD), and high-resolution transmission electron microscopy (HRTEM). The petcoke model consisted of 56 hydrocarbon molecules, stacked, curved, and planar. The element content, functional groups, aromaticity, stacking extent, etc., of the model corresponded to the actual Qingdao petcoke.

https://doi.org/10.1021/acsomega.3c01446
ACS Omega 2023, 8, 18140−18150

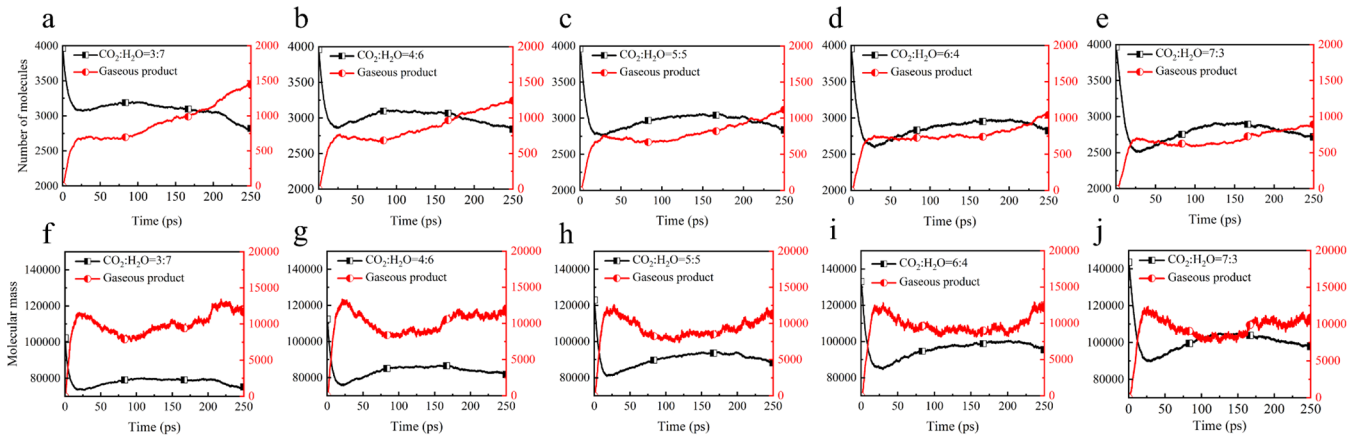

Figure 2. Number of all gaseous products molecules under CO_2/H_2O ratios of (a) 3:7, (b) 4:6, (c) 5:5, (d) 6:4, and (e) 7:3, and molar mass of all gaseous products under CO_2/H_2O ratios of (f) 3:7, (g) 4:6, (h) 5:5, (i) 6:4, and (j) 7:3.

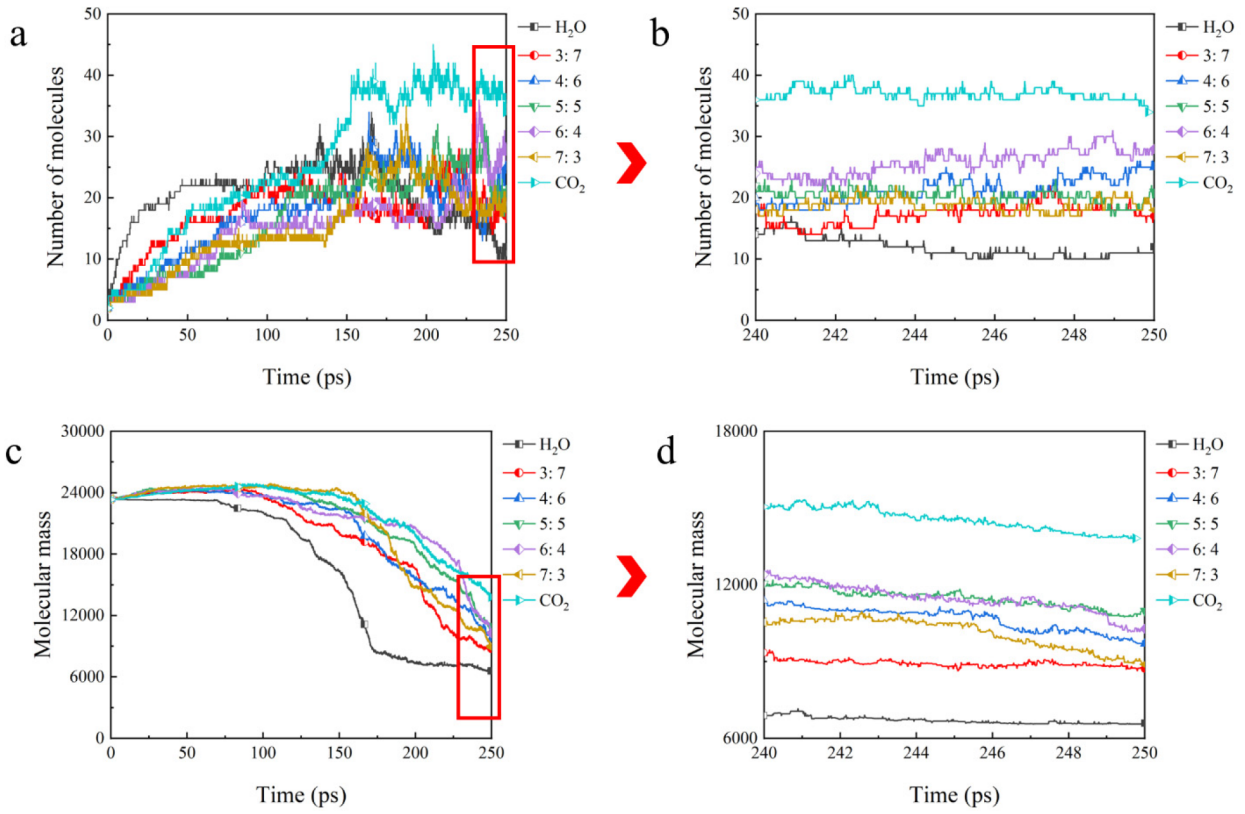

Figure 3. Comparison of (a,b) number of molecules and (c,d) molecular mass of all nongas products.

2.2. ReaxFF MD Simulation Parameters. The potential function (eq 1) of ReaxFF covers bond energy (E_{bond}), overcoordinated atom in the energy contribution (E_{over}), three-body valence angle strain energy (E_{angle}), angle strain energy (E_{angle}), penalty energy (E_{pen}), torsion conjugation energy (E_{conj}), four-body torsional angle strain energy (E_{tors}), Coulomb interaction ($E_{Coulomb}$), and nonbonded van der Waals interaction ($E_{vdWaals}$).

$$E_{system} = E_{bond} + E_{over} + E_{under} + E_{angle} + E_{val} + E_{pen} + E_{conj} + E_{tors} + E_{Coulomb} + E_{vdWaals} \quad (1)$$

The ReaxFF MD simulation was carried out using the $ReaxFF_{-CHONSSi}$ force field in the Amsterdam Density Functional (ADF) software package. The constructed petcoke model was located at the center of the 146 × 146 × 146 Å cell. The bond order cutoff was selected as 0.3 for graphs and 0.001 for valency angles and torsion angles. The temperature was 3000 K to ensure that the reaction would be completed within an acceptable time. The time step was selected as 0.25 ps to better observe the transformation of S and N elements. To explore the relevance and regularity between petcoke gasification productivity and the CO_2/H_2O ratio, the simulations were carried out at 3000 K with the ratio of CO_2 and H_2O being its only variable (CO_2/H_2O ratio was 3:7, 4:6, 5:5, 6:4, and 7:3).

https://doi.org/10.1021/acsomega.3c01446
ACS Omega 2023, 8, 18140−18150

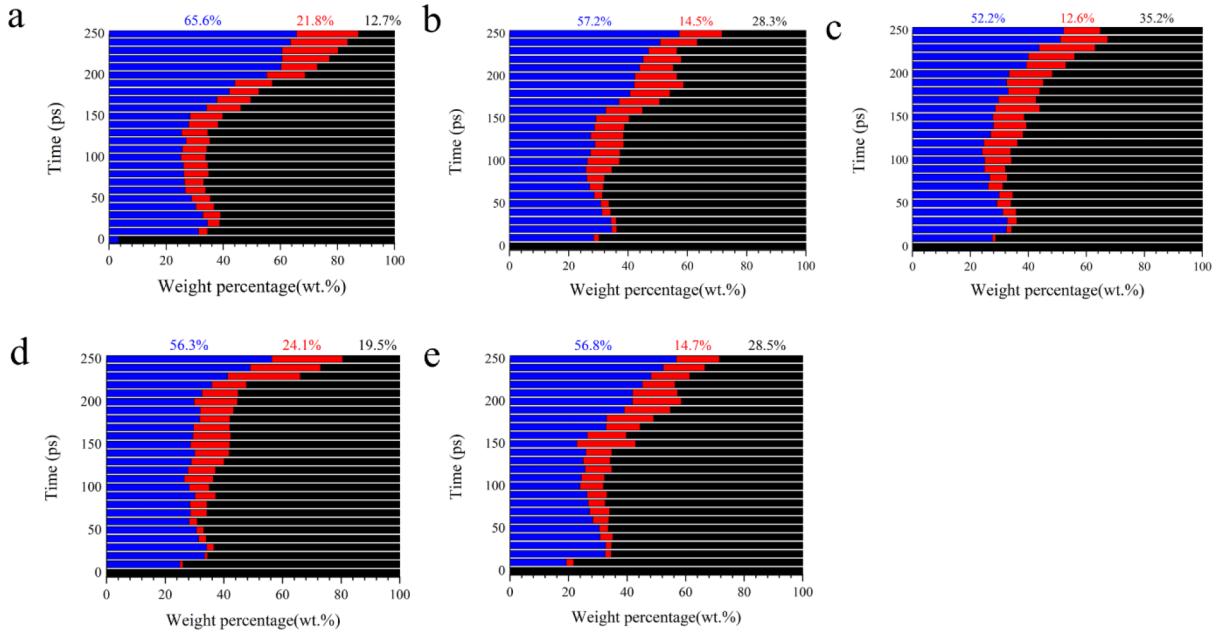

Figure 4. Distribution of gas, tar (C_5−C_{40}), and coke (C_{41+}) under CO_2/H_2O ratios of (a) 3:7, (b) 4:6, (c) 5:5, (d) 6:4, and (e) 7:3. The blue bar represents the weight percentage of gas, red for tar and black for coke.

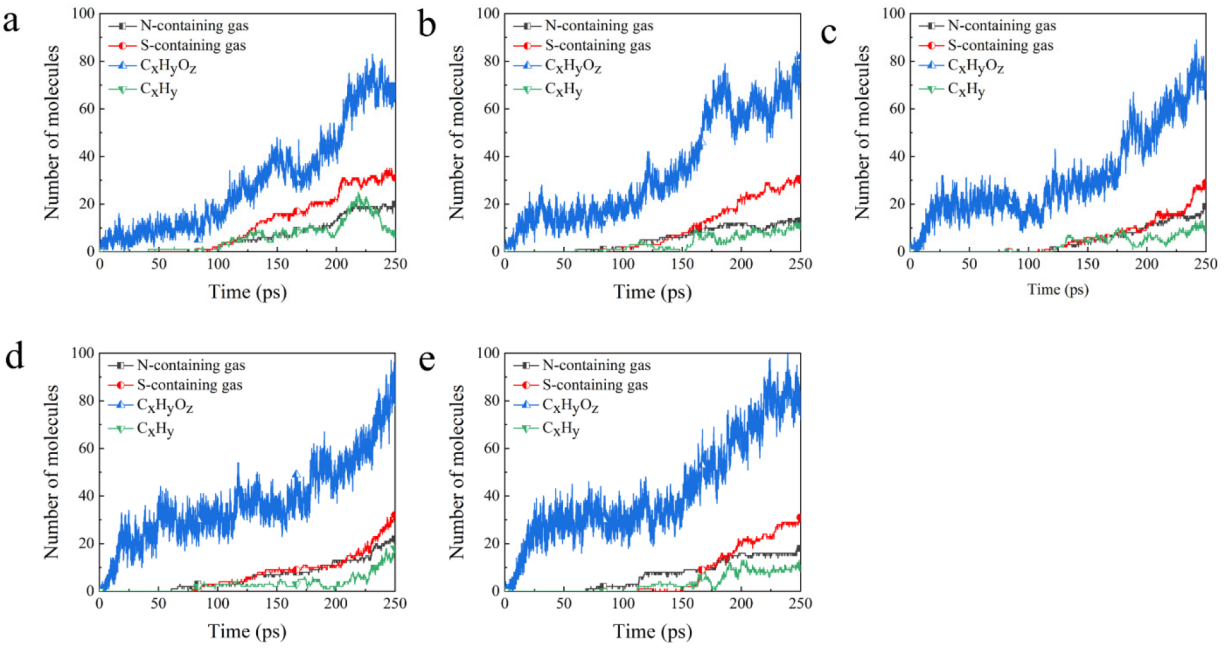

Figure 5. Number of main gaseous product molecules under CO_2/H_2O ratios of (a) 3:7, (b) 4:6, (c) 5:5, (d) 6:4, and (e) 7:3.

3. RESULTS AND DISCUSSION

3.1. Comparison of Gas and Nongas Product Yields under Different CO_2/H_2O Ratios. Figure 1 presents the separation and dispersion of the petcoke particle and its fragments under different CO_2/H_2O ratios, as exemplified by the 5:5 ratio. To exclude the interference of CO self-reactions, C_xO_y molecules such as C_2O_2 were ignored.[5] Figure 2a−e shows the evolution of the total molecular number and mass of the raw materials (CO_2 and H_2O) and gaseous products. A dramatic increase in gaseous products was observed before their generation rate slowed down, while the total number of CO_2 and H_2O molecules exhibited an opposite behavior. This tendency was closely connected with the decomposition of H_2O. It was found that a considerable amount of H_x and H_xO_y (Figure S1) molecules was produced at the early stage of gasification due to the rapid decomposition of H_2O under extremely high temperatures. These molecules were consumed quickly, resulting in a decelerated generation of all gas products. Consequently, as shown in Figure 2a−e, a tendency of gentle decline emerged after the rapid growth in product quantity. After this smooth transition stage, many smaller product molecules appeared due to the sufficient decomposition of petcoke particles aided by abundant reductive agents. Hence, the number of gas molecules increased at the final stage, despite the consumption of reductive agents. Meanwhile, both the raw material and gaseous product curves

https://doi.org/10.1021/acsomega.3c01446
ACS Omega 2023, 8, 18140−18150

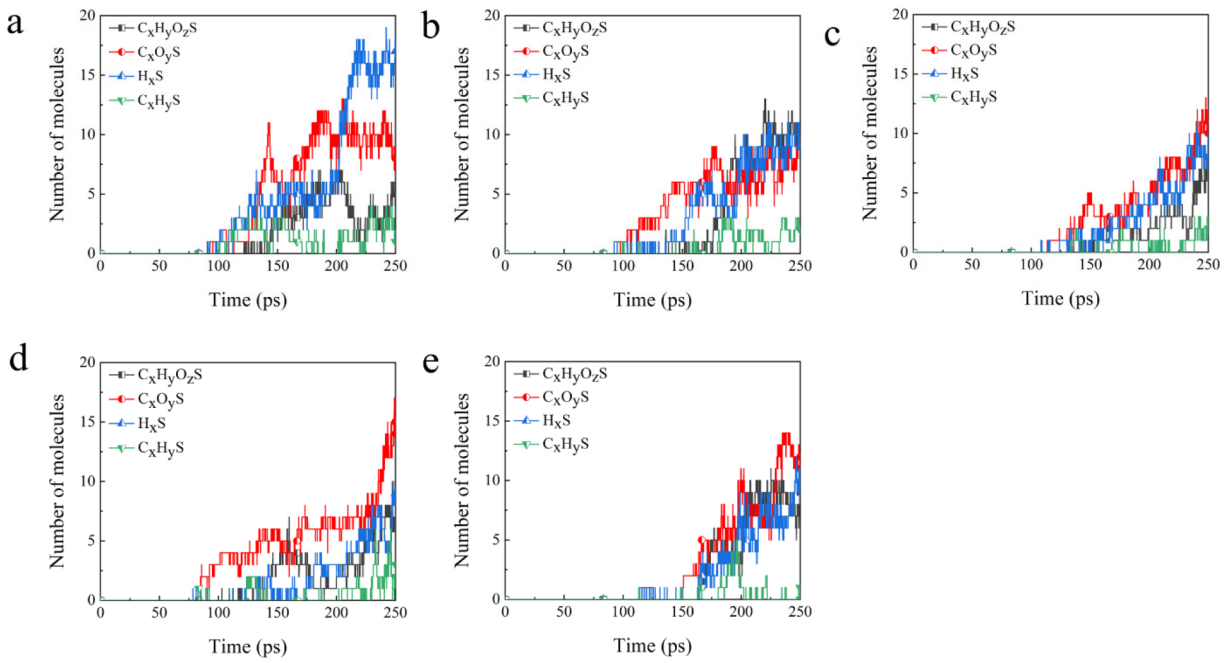

Figure 6. Number of main S-containing gas species under CO_2/H_2O ratios of (a) 3:7, (b) 4:6, (c) 5:5, (d) 6:4, and (e) 7:3.

moved down. The total gas product molecules decreased from 1500 (Figure 2a) to less than 1000 (Figure 2e) at the end of the simulation. Such results were similar to those in the previous report in which adding CO_2 into the CO_2/H_2O mixture was found to be capable of decelerating the gasification reaction.[33]

As shown in Figure 2f–j, the tendency of the single molecular mass curve was identical to that of the molecular number. Differently, as the CO_2/H_2O ratio increased from 3:7 (Figure 2f) to 7:3 (Figure 2j), the CO_2/H_2O curve increased owing to the larger molar mass of CO_2. At the final stage of gasification, the molecular masses of all groups were close to each other (all reached 12000), while the molecular number decreased as the CO_2 content in gasification agent increased. Therefore, it could be inferred that the increase of the CO_2/H_2O ratio would generate a higher carbon content in gaseous products. Such a phenomenon is adverse to the petcoke gasification process because products such as CO, CH_4, and H_2 (syngas) are favorable for energy applications.[34]

Figure 3 demonstrates the comparison of molecular number and molecular mass during gasification aided by H_2O, CO_2, and their mixture. The positive effect that H_2O has on gasification is further confirmed. Figure 3a,c shows that, as the reaction proceeded, the number of nongas molecules increased while their molecular mass decreased, indicating the decomposition of the petcoke molecule. Noticeably, in Figure 3a,c, the CO_2/H_2O gasification curves were located in the middle of H_2O gasification (CO_2/H_2O ratio 0:10) and CO_2 gasification (CO_2/H_2O ratio 10:0). This phenomenon is further demonstrated in Figure 3b,d. The curves for CO_2/H_2O gasification moved up as CO_2 content increased. Although all seven groups reached an equilibrium state in the last 10 ps of the reaction, Figure 3c indicates that the more H_2O participates in gasification, the faster the equilibrium state was achieved. For the H_2O gasification system, the reaction was almost completed at 170 ps. Moreover, Figure 4 depicts the distribution of gas, tar, and coke during different gasification stages. It was clear that a higher CO_2/H_2O ratio resulted in an incomplete gasification extent. The gas content dropped from 66 to 57% while coke multiplied by over two times as the CO_2/H_2O ratio increased from 3:7 (Figure 3a) to 7:3 (Figure 3e). Based on the findings mentioned above, it could be verified that H_2O was more helpful in boosting the extent of gasification.

3.2. S/N Removal Efficiency and the Evolution of S/N-Containing Species. The molecular number of S/N-containing gas and main product species ($C_xH_yO_z$ and C_xH_y) are presented in Figure 5. In all five graphs, the number of product molecules grew over time. Despite the CO_2/H_2O ratio, the molecular number of all four major product types ended up close. The most produced molecule species was $C_xH_yO_z$ (70–80 molecules), and the least was C_xH_y (~10 molecules), while the final numbers of S- and N-containing molecules were around 30 and 20, respectively. This implied that desulfurization and denitrification reactions could complete within 250 ps regardless of CO_2/H_2O ratio. Nevertheless, from Figure 5a–e, the initial appearance of S-containing gas seemed to be delayed as the CO_2/H_2O ratio increased. Figure 5a (CO_2/H_2O ratio 3:7) shows that desulfurization was half completed at 150 ps and approached equilibrium at 200 ps. In stark contrast, in Figure 5e (CO_2/H_2O ratio 7:3), the number of S-containing molecules only started to increase prominently after 150 ps. In the other three groups (CO_2/H_2O ratios 4:6, 5:5, and 6:4), S-containing products appeared between 80 and 100 ps. It could be concluded that the generation rate of S-containing gas was slower when the CO_2/H_2O ratio was 7:3 compared to when it was 3:7.

Figure 6 shows the positive effect of H_2O on the evolution of S-containing gas as CO_2/H_2O gradually increased. When the CO_2/H_2O ratio was 3:7 (Figure 6a), a considerable amount of four kinds of S-containing gas species ($C_xH_yO_zS$, C_xO_yS, H_xS, and C_xH_yS) were generated before 100 ps. Comparatively, in Figure 6e, none of the S-containing species exceeded 5 molecules before 150 ps under a CO_2/H_2O ratio of 7:3. Apart from accelerating the generation of S-containing gas, the

https://doi.org/10.1021/acsomega.3c01446
ACS Omega 2023, 8, 18140–18150

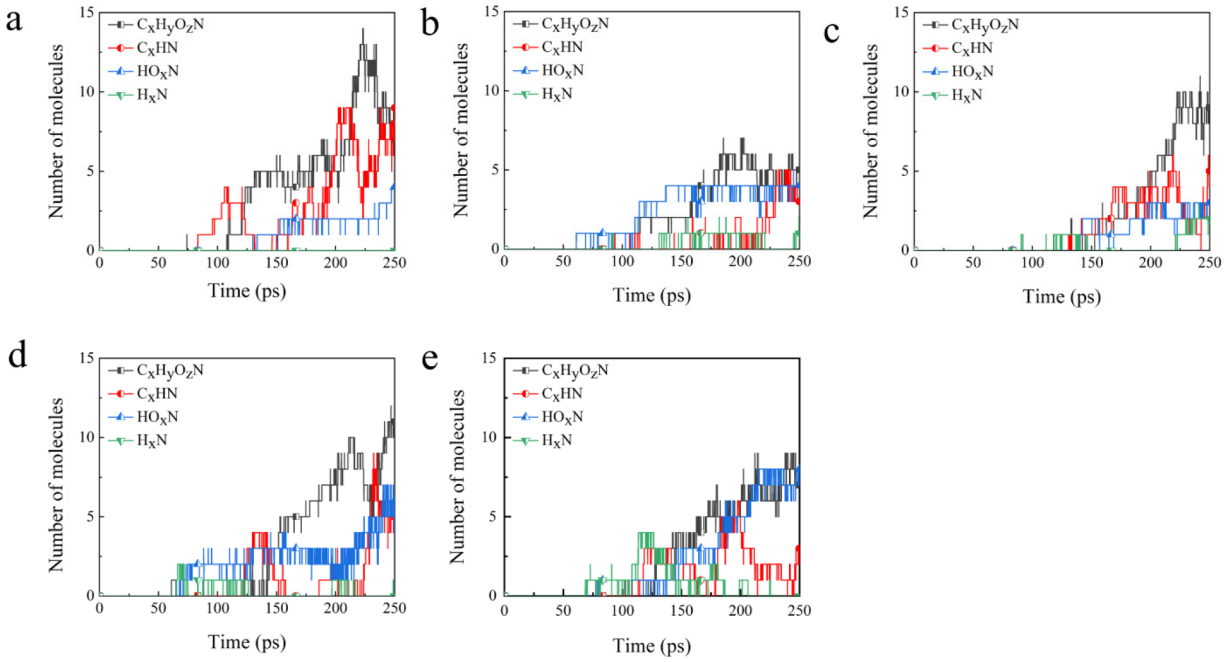

Figure 7. Number of main N-containing gas species under CO_2/H_2O ratios of (a) 3:7, (b) 4:6, (c) 5:5, (d) 6:4, and (e) 7:3.

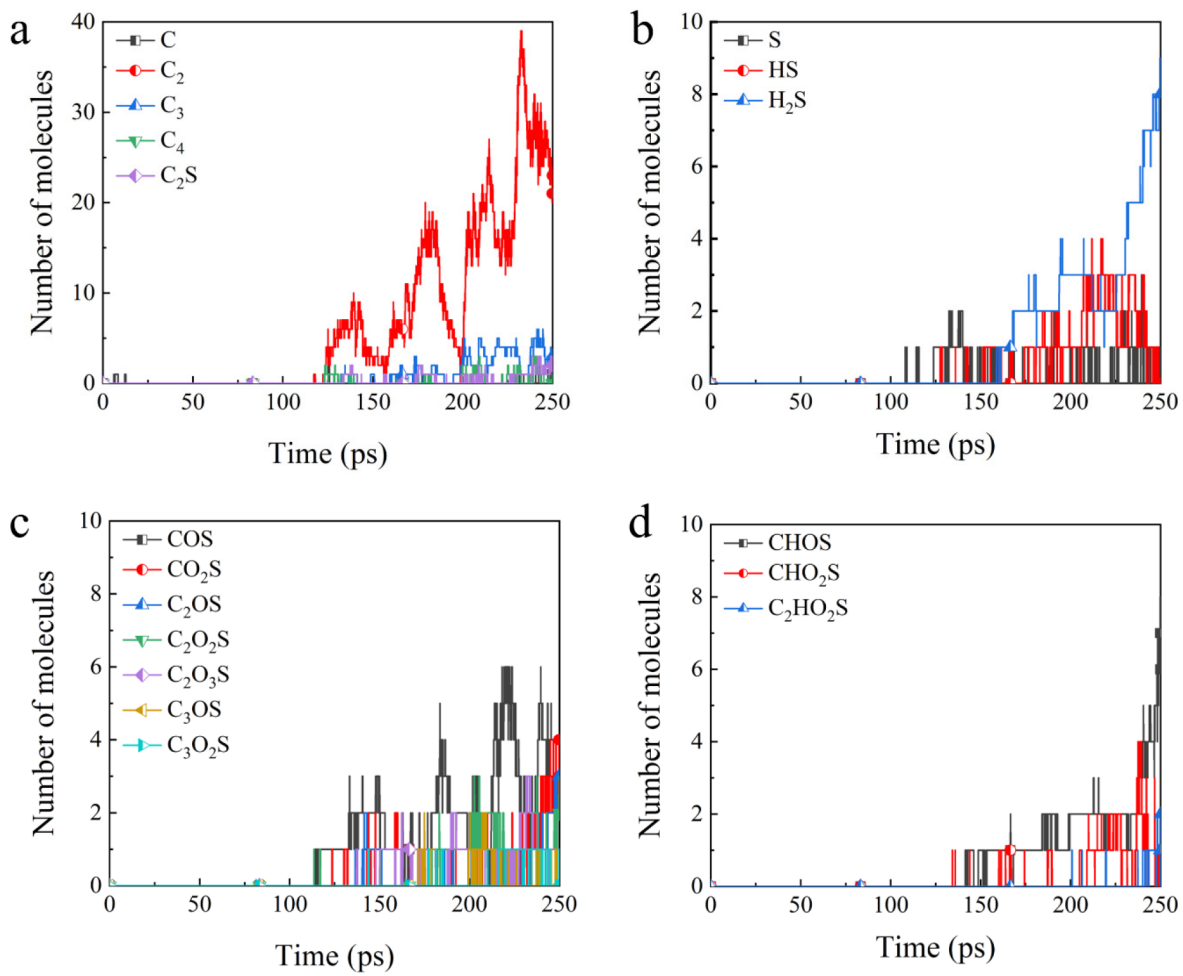

Figure 8. Sulfur-containing gaseous products (a) C_2S and C_x ($x < 5$) species; (b) H_xS ($x = 0,1,2$); (c) C_xO_yS; (d) $C_xH_yO_2S$ during petcoke gasification under the CO_2/H_2O ratio of 5:5.

https://doi.org/10.1021/acsomega.3c01446
ACS Omega 2023, 8, 18140−18150

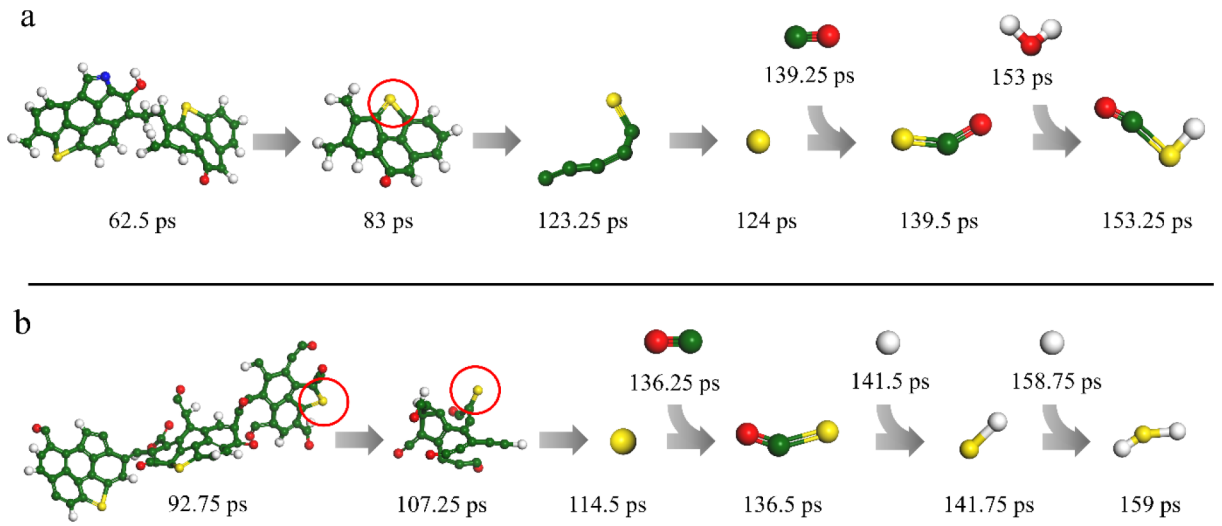

Figure 9. Sulfur removal mechanism during petcoke CO_2/H_2O gasification (green for C atoms, white for H atoms, red for O atoms, yellow for S atoms and blue for N atoms): typical formation path of (a) CHOS and (b) H_2S.

decrease of the CO_2/H_2O ratio also influenced the percentage of the H-abundant H_xS species. The number of H_xS produced at the end of the reaction was 17 and 10 as the CO_2/H_2O ratio increased from 3:7 to 7:3. From Figure 6a−c, the H_xS curves exhibited a dramatic downward trend but remained unchanged in Figure 6d,e because of the limited S atoms (47 in total). This indicates that the predominance of H_xS species in S-containing products was replaced by the high carbon-containing C_xO_yS. Therefore, the higher the CO_2/H_2O ratio, the more the amount of high carbon-containing gaseous products.

Figure 7 presents the change of N-containing gas under different CO_2/H_2O ratios. In stark contrast to S-containing gas, the amount of N-containing gas had a mere correlation with the CO_2/H_2O ratio. From Figure 5 and Figure 7, it was found that the initiation of the denitrification reaction was not delayed as desulfurization was. From Figure 7a−e, N-containing gas emerged around 75 ps. Furthermore, no obvious fluctuation in the generation rate of N-containing gas was observed as the CO_2/H_2O ratio increased from 3:7 to 7:3. The major existing form of N element in the product was $C_xH_yO_zN$ (x included 0). Not less than 5 $C_xH_yO_zN$ molecules were produced at 250 ps in all five groups, with the highest being 14 (Figure 7a), which dramatically surpassed the production of H_xN. Notice that the petcoke model applied in this research was limited in scale, especially for the N element (only 24 N atoms in total). Consequently, detailed regularity for the transformation of the N element was difficult to observe. The above findings imply that in petcoke CO_2/H_2O gasification, a low CO_2/H_2O ratio is preferred for S removal. A high H_2O proportion in the gasifier helps to improve the extent of gasification and the conversion of environmentally hazardous S, but the CO_2/H_2O ratio has a mere influence on N removal.

3.3. Mechanism Analysis for Desulfurization and Denitrification. To obtain a comprehensive understanding of the synergistic effect of the CO_2/H_2O mixture in petcoke gasification, the reaction path needs to be analyzed. To ensure an equal influence of H_2O and CO_2, results of 5:5 CO_2/H_2O ratio simulation were chosen for the mechanism exploration. Figure 8 demonstrates the distribution of all S-containing gas produced in the simulation. The removed S atoms mostly existed in the form of C_xO_yS, H_xS, and $C_xH_yO_zS$ under the reductive gasification environment. COS, H_2S, and CHOS dominated among all the S-containing products produced in gasification. From Figure 8b, it was found that both the number of S and HS decreased after reaching their peaks. Differently, the number of H_2S increased rapidly at the last 30 ps of the reaction. Such a difference indicates that the generation of H_2S involved S and HS. Additionally, in Figure 8b, the product S emerged dramatically ahead of HS, implying the transformation from S to HS. The inferred relationship among S, HS, and H_2S could be expressed as eq 2. Figure 8c shows that the COS (Figure 8c) fluctuated several times. It was determined that the conversion from COS to CHOS (eq 3) was responsible for the fluctuation of COS and the rapid increase of CHOS.

$$\text{thiophene-S(petcoke)} \rightarrow \text{R-S} \rightarrow \text{S} + \text{H} \rightarrow \text{H}_2\text{S} \quad (2)$$

$$\text{thiophene-S(petcoke)} \rightarrow \text{R-S} \rightarrow \text{S} + \text{CO} \rightarrow \text{C}_x\text{O}_y\text{S} + \text{H}_x/\text{H}_x\text{O}_y \rightarrow \text{C}_x\text{H}_y\text{O}_z \quad (3)$$

During carbon-based material gasification, pyrolysis often takes place before or concurrent with other reactions involving gasifiers.[35−37] Large raw material particles undergo complicated pyrolysis reactions and break down to produce tar, inorganic gas, and other volatile products. In petcoke gasification by the CO_2/H_2O mixture, the S element was found to detach first in much smaller molecules and via pyrolysis. Under high temperatures, these S-containing small molecules continued to decompose and produce S atoms. This process paved the way for the production of major S-containing gas such as CHOS, COS, and H_2S because S atoms could easily react with CO and H. As is shown in Figure 9a, in a typical formation of CHOS, large S-containing particles broke down gradually before the eventual detachment of thiophene-S at 124 ps. Shortly after 15.25 ps, the S atom was reduced by the CO molecule to form COS. At 153.25 ps, the COS molecule was transformed to CHOS by H in the H_2O molecule. The COS molecules involved in this process acted as both the major product of gasification and an important intermediate to generate CHOS. Similarly, during the formation of H_2S presented in Figure 9b, a single S atom

https://doi.org/10.1021/acsomega.3c01446
ACS Omega 2023, 8, 18140−18150

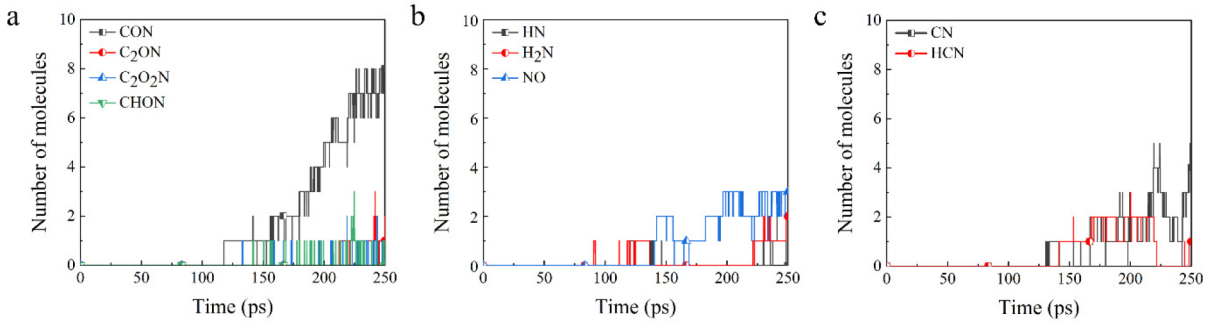

Figure 10. Nitrogen-containing gaseous products (a) C_xO_yN and CHON; (b) H_xN and NO; (c) HCN and CN during petcoke gasification under the CO_2/H_2O ratio of 5:5.

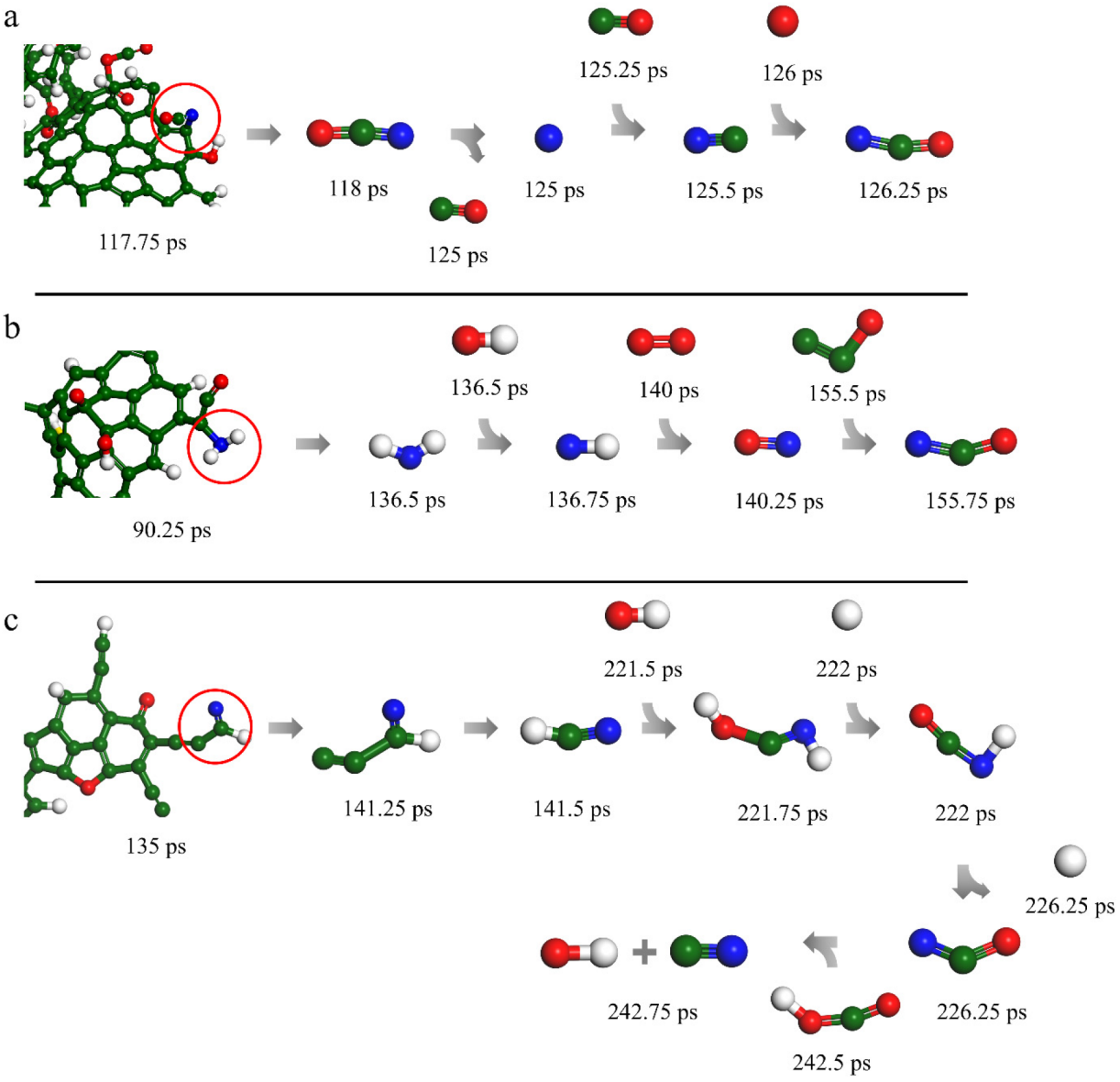

Figure 11. Nitrogen removal mechanism during petcoke CO_2/H_2O gasification (green for C atoms, white for H atoms, red for O atoms, yellow for S atoms and blue for N atoms): (a) direct generation of CON and its conversion; (b) formation path of CON; and (c) interconversion of different N-containing products.

was generated during pyrolysis. The S atom combined with CO to form COS at 136.5 ps. At 141.75 ps, the CO in COS was substituted by the more competitive H atoms to produce HS and, finally, H_2S.

https://doi.org/10.1021/acsomega.3c01446
ACS Omega 2023, 8, 18140−18150

Nevertheless, in Figure 10, N atoms were distributed in various kinds of gas molecules including C_xO_yN, $H_{1-2}N$, $H_{0-1}CN$, CHON and NO. The variety in N-containing products stemmed from the distinctive N transfer behavior compared with S. In Figure 10a, the predominant CON presented a rapidly increasing trend from 150 to 200 ps. There were 8 CON molecules at the end of gasification, while no more than 3 molecules were produced for C_2ON, C_2O_2N, and CHON each. However, the evolution of N-containing products such as CON and CHON did not show the similar correlation with each other as COS and CHOS did. For example, in Figure 10c, CHN was first generated at around 140 ps, and its quantity began to decline at 220 ps. Nevertheless, the number of CN experienced 2 peaks and maintained an increasing tendency at 250 ps. Therefore, it could be speculated from Figure 10 that pyrolysis and mutual conversion were attributed to the variety of N-containing products rather than the reductive CO, H, and OH. And because the number of CON far exceeded other N-containing gas products, most N atoms would eventually exist in the form of CON.

The detailed N removal path is shown in Figure 11. The complexity of N transformation varies among each path. In Figure 11a, CON detached from petcoke particle as a whole at 118 ps. It was quickly stabilized with the aid of CO and O within 8.25 ps. However, in Figure 11b, distinct from the generation path of H_2S (Figure 9b), H_2N appeared directly via pyrolysis. Instead of combining one H atom to form NH_3 molecule each time, H_2N reacted with OH to produce HN. Then the HN reacted with O_2 and C_2O successively to produce CON. Furthermore, Figure 11c depicts a much more complicated denitrification path. Most of the main N-containing gaseous products were involved, including HCN, CHON, CON, CO_2N, etc. In detail, the N atom came out in the form of HCN. The HCN reacted with HO and H successively. During the transformation process, CH_2ON, CHON, and CON were generated. At 242.5 ps, the CON molecule reacted with another gasification product, CHO_2, and was finally converted into CN. The denitrification paths could also be expressed as eq 4−6.

$$\text{pyrrole-/pyridine-N(pyrolysis)} \rightarrow \text{CON} \quad (4)$$

$$\text{pyrrole-/pyridine-N(pyrolysis)} \rightarrow H_2N + OH/O_2 \rightarrow NO + C_xO \rightarrow CON \quad (5)$$

$$\text{pyrrole-/pyridine-N(pyrolysis)} \rightarrow HCN + OH/H \rightarrow CHON \rightarrow CON + CHO_2 \rightarrow CN \quad (6)$$

Overall, CO_2/H_2O ratio impacts on desulfurization more than denitrification. This phenomenon can be explained by two main factors. On the one hand, the S-removal path was simpler than N-removal due to its dependence on the reductive CO and H. S element mostly detached from petcoke via pyrolysis as a single atom. Then the S atoms reacted with the reductive CO and H. As a result, almost all the S-containing gas products belonged to one of the C_xO_yS, $C_xH_yO_zS$, or H_xS or species. In comparison, single N atoms were merely observed to be separated from the petcoke particle. N-containing products such as CON could directly originate from petcoke pyrolysis. Besides, through reacting with CO, H and other gasification products, including CHO_2, denitrification products could be converted from one to another. On the other hand, major gasification agents could react with each other. As gasifiers, instead of directly participating in the reaction, the CO_2/H_2O mixture aided petcoke gasification by generating the reductive CO, H_x, and OH. Interactions among these agents could not be neglected. Two typical reactions were the water gas shift reaction (eq 7) and the steam-gasification reaction (eq 8). In both reactions, the active H_2O was reduced to produce the reductive H_2, while CO_2 acted as the product. Consequently, the more the H_2O, the more the reducing agents were generated. According to the previous analysis, H/H_2 was able to react with COS to generate H_2S or CHOS during desulfurization (Figure 8b). Hence, the increase in H_2O content could generate the increase of H_x and therefore accelerate the S removal process.

$$CO + H_2O \rightarrow CO_2 + H_2 \ (\text{water–gas shift reaction}) \quad (7)$$

$$C + H_2O \rightarrow CO + H_2 \ (\text{steam-gasification reaction}) \quad (8)$$

4. CONCLUSION

The regularity of petcoke CO_2/H_2O gasification under different CO_2/H_2O ratios was explored via ReaxFF MD simulations. The simulation results revealed the influence of the CO_2/H_2O ratio on the gasification, desulfurization, and denitrification extent. A higher H_2O content in gasifiers dramatically facilitated gasification and desulfurization, while denitrification was not significantly influenced. By increasing H_2O content, the remaining coke in the product was reduced from 28.5 to 12.7%, and the gas yield increased from 56.8 to 65.6%. For desulfurization, thiophene-S experienced more than 100 ps to detach from solid particles in the form of S atoms. The single S atoms combined with either CO or H to produce COS and HS. The abundant HS and COS were further transformed into H_2S and CHOS by the reductive H. The denitrification mechanism was found diversified. Apart from reacting with CO_2 and H_2O, interconversion among N-containing products occurred frequently. With the aid of H and CO, CHON was transferred into CON and H_2N into HN. Non-N/S-containing gas such as C_2O and CHO_2 could also react with NO and CON to produce CON and CN, respectively. Direct reduction of N-containing gases by H and CO was infrequent. Consequently, the N-removal process was little affected by the CO_2/H_2O ratio and the composition of N-containing gas was complicated. The results of this study provide constructive guidance for the future application of petcoke gasification with mixed agents.

■ ASSOCIATED CONTENT

Supporting Information

The Supporting Information is available free of charge at https://pubs.acs.org/doi/10.1021/acsomega.3c01446.

Figure S1 showing the number of (a) H_2O molecules and (b) H_xO_y species under different CO_2/H_2O ratios (PDF)

■ AUTHOR INFORMATION

Corresponding Authors

Qiuyun Mao − *Department of Educational Science, Hunan First Normal University, Changsha 410205, China*; Email: 137477993@qq.com

https://doi.org/10.1021/acsomega.3c01446
ACS Omega 2023, 8, 18140−18150

Qifan Zhong − *School of Metallurgy and Environment, Central South University, Changsha 410083, China;* orcid.org/0000-0003-4963-0516; Email: 348259246@qq.com

Authors

Jiazhuang Tian − *College of Chemistry and Chemical Engineering, Central South University, Changsha 410083, China*

Zihan You − *School of Metallurgy and Environment, Central South University, Changsha 410083, China*

Complete contact information is available at: https://pubs.acs.org/10.1021/acsomega.3c01446

Author Contributions

Conceptualization, Q.Z. and Q.M.; methodology, Q.Z.; formal analysis, J.T.; writing—original draft preparation, J.T.; writing—review and editing, Z.Y. and Q.Z.; supervision, Q.Z.

Notes

The authors declare no competing financial interest.

■ ACKNOWLEDGMENTS

This work was supported by the National Natural Science Foundation of China (No. 52174338), Natural Science Foundation of Hunan Province, China (Nos. 2022JJ20086 and 2021JJ30796), and Central South University Innovation-Driven Research Programme (No. 2023CXQD005). This work was supported in part by the High-Performance Computing Center of Central South University.

■ REFERENCES

(1) Murthy, B. N.; Sawarkar, A. N.; Deshmukh, N. A.; Mathew, T.; Joshi, J. B. PETROLEUM COKE GASIFICATION: A REVIEW. *Can. J. Chem. Eng.* **2014**, *92* (3), 441−468.

(2) Shan, Y.; Guan, D.; Meng, J.; Liu, Z.; Schroeder, H.; Liu, J.; Mi, Z. Rapid growth of petroleum coke consumption and its related emissions in China. *Appl. Energy* **2018**, *226*, 494−502.

(3) Liu, J.; Mao, Q.; Wang, G.; Xiao, J.; Zhong, Q. Removal and transformation mechanisms of nitrogen and sulfur in petcoke supercritical water gasification via ReaxFF simulation. *Mol. Simul.* **2022**, *48* (3), 209−220.

(4) Zhong, Q.; Zhang, Y.; Shabnam, S.; Xiao, J.; Van Duin, A. C.; Mathews, J. P. Reductive gaseous (H_2/NH_3) desulfurization and gasification of high-sulfur petroleum coke via reactive force field molecular dynamics simulations. *Energy Fuels* **2019**, *33* (9), 8065−8075.

(5) Zhong, Q.; Zhang, Y.; Shabnam, S.; Mao, Q.; Xiao, J.; van Duin, A. C.; Mathews, J. P. ReaxFF MD simulations of petroleum coke CO2 gasification examining the S/N removal mechanisms and CO/CO_2 reactivity. *Fuel* **2019**, *257*, 116051.

(6) Edwards, L. C.; Neyrey, K. J.; Lossius, L. P. A review of coke and anode desulfurization. *Essential readings in light metals* **2016**, 130−135.

(7) Wang, J.; Anthony, E. J.; Abanades, J. C. Clean and efficient use of petroleum coke for combustion and power generation. *Fuel* **2004**, *83* (10), 1341−1348.

(8) Al-Haj-Ibrahim, H.; Morsi, B. I. Desulfurization of petroleum coke: a review. *Ind. Eng. Chem. Res.* **1992**, *31* (8), 1835−1840.

(9) Lukasiewicz, S. J.; Johnson, G. C. Desulfurization of petroleum coke. *Ind. Eng. Chem.* **1960**, *52* (8), 675−677.

(10) El-Kaddah, N.; Ezz, S. Y. Thermal desulphurization of ultra-high-sulphur petroleum coke. *Fuel* **1973**, *52* (2), 128−129.

(11) Liu, K.; Yuan, Z.; Shi, C.; Zhao, H.; Wang, H. Effect of CaO-SiO_2-FeO slag system on coal gasification reaction in CO_2-Ar atmosphere and kinetic analysis. *J CO_2 Utilization* **2022**, *56*, 101850.

(12) Echegaray, M.; García, D. Z.; Mazza, G.; Rodriguez, R. Air-steam gasification of five regional lignocellulosic wastes: exergetic evaluation. *Sustainable Energy Technologies and Assessments* **2019**, *31*, 115−123.

(13) Midilli, A.; Kucuk, H.; Topal, M. E.; Akbulut, U.; Dincer, I. A comprehensive review on hydrogen production from coal gasification: Challenges and Opportunities. *Int. J. Hydrogen Energy* **2021**, *46* (50), 25385−25412.

(14) Janajreh, I.; Adeyemi, I.; Raza, S. S.; Ghenai, C. A review of recent developments and future prospects in gasification systems and their modeling. *Renew. Sust. Energy Rev.* **2021**, *138*, 110505.

(15) Zhao, P. J.; Ma, C.; Wang, J. T.; Qiao, W. M.; Ling, L. C. Almost total desulfurization of high-sulfur petroleum coke by Na_2CO_3-promoted calcination combined with ultrasonic-assisted chemical oxidation. *New Carbon Mater.* **2018**, *33* (6), 587−594.

(16) Rana, R.; Nanda, S.; Maclennan, A.; Hu, Y.; Kozinski, J. A.; Dalai, A. K. Comparative evaluation for catalytic gasification of petroleum coke and asphaltene in subcritical and supercritical water. *J. Energy Chem.* **2019**, *31*, 107−118.

(17) Vrinat, M. The kinetics of the hydrodesulfurization process-a review. *Applied Catalysis* **1983**, *6* (2), 137−158.

(18) Harris, D. J.; Smith, I. W. Intrinsic reactivity of petroleum coke and brown coal char to carbon dioxide, steam and oxygen. *Symposium (International) on Combustion*; Elsevier, 1991; Vol. *23*, pp 1185−1190.

(19) Xiao, J.; Zhang, Y.; Zhong, Q.; Li, F.; Huang, J.; Wang, B. Reduction and desulfurization of petroleum coke in ammonia and their thermodynamics. *Energy Fuels* **2016**, *30* (4), 3385−3391.

(20) Alam, M.; Wijayanta, A.; Nakaso, K.; Fukai, J. Syngas Production from Coal Gasification with CO_2 Rich Gas Mixtures. *International Symposium on Coal Combustion*; Springer, 2011; pp 1103−1108.

(21) Jeremiáš, M.; Pohořelý, M.; Svoboda, K.; Manovic, V.; Anthony, E. J.; Skoblia, S.; Beňo, Z.; Šyc, M. Gasification of biomass with CO_2 and H_2O mixtures in a catalytic fluidised bed. *Fuel* **2017**, *210*, 605−610.

(22) Thanapal, S. S.; Annamalai, K.; Sweeten, J. M.; Gordillo, G. Fixed bed gasification of dairy biomass with enriched air mixture. *Appl. Energy* **2012**, *97*, 525−531.

(23) Kislov, V.; Glazov, S.; Salgansky, E.; Kolesnikova, Y.; Salganskaya, M. Coal gasification by a mixture of air and carbon dioxide in the filtration combustion mode. *Combustion, Explosion, and Shock Waves* **2016**, *52* (3), 320−325.

(24) Sharma, P.; Gupta, B.; Pandey, M. Hydrogen Rich Product Gas from Air-Steam Gasification of Indian Biomasses with Waste Engine Oil as Binder. *Waste and Biomass Valorization* **2022**, *13* (6), 3043−3060.

(25) Huo, W.; Zhou, Z.; Chen, X.; Dai, Z.; Yu, G. Study on CO_2 gasification reactivity and physical characteristics of biomass, petroleum coke and coal chars. *Bioresource technology* **2014**, *159*, 143−149.

(26) Wang, M.; Wan, Y.; Guo, Q.; Bai, Y.; Yu, G.; Liu, Y.; Zhang, H.; Zhang, S.; Wei, J. Brief review on petroleum coke and biomass/coal co-gasification: Syngas production, reactivity characteristics, and synergy behavior. *Fuel* **2021**, *304*, 121517.

(27) Zhou, T.; Ge, L.; Li, Q.; Yang, L.; Mai, L.; Huang, J.; Wang, Y.; Xu, C. Combustion and gasification properties of petroleum coke and its pyrolytic semi-coke. *Energy* **2023**, *266*, 126414.

(28) Castro-Marcano, F.; Kamat, A. M.; Russo, M. F.; van Duin, A. C. T.; Mathews, J. P. Combustion of an Illinois No. 6 coal char simulated using an atomistic char representation and the ReaxFF reactive force field. *Combust. Flame* **2012**, *159* (3), 1272−1285.

(29) Bhoi, S.; Banerjee, T.; Mohanty, K. Molecular dynamic simulation of spontaneous combustion and pyrolysis of brown coal using ReaxFF. *Fuel* **2014**, *136*, 326−333.

(30) Li, X. X.; Zheng, M.; Ren, C. X.; Guo, L. ReaxFF Molecular Dynamics Simulations of Thermal Reactivity of Various Fuels in Pyrolysis and Combustion. *Energy Fuels* **2021**, *35* (15), 11707−11739.

(31) Xiao, J.; Zhong, Q. F.; Li, F. C.; Huang, J. D.; Zhang, Y. B.; Wang, B. J. Modeling the Change of Green Coke to Calcined Coke Using Qingdao High-Sulfur Petroleum Coke. *Energy Fuels* **2015**, *29* (5), 3345−3352.
(32) Zhong, Q. F.; Mao, Q. Y.; Zhang, L. Y.; Xiang, J. H.; Xiao, J.; Mathews, J. P. Structural features of Qingdao petroleum coke from HRTEM lattice fringes: Distributions of length, orientation, stacking, curvature, and a large-scale image-guided 3D atomistic representation. *Carbon* **2018**, *129*, 790−802.
(33) Trommer, D.; Steinfeld, A. Kinetic modeling for the combined pyrolysis and steam gasification of petroleum coke and experimental determination of the rate constants by dynamic thermogravimetry in the 500- 1520 K range. *Energy Fuels* **2006**, *20* (3), 1250−1258.
(34) Li, F.; Fan, L.-S. Clean coal conversion processes-progress and challenges. *Energy Environ. Sci.* **2008**, *1* (2), 248−267.
(35) Dutta, S.; Wen, C.; Belt, R. Reactivity of coal and char. 1. In carbon dioxide atmosphere. *Industrial & Engineering Chemistry Process Design and Development* **1977**, *16* (1), 20−30.
(36) Zhong, Q.; Mao, Q.; Xiao, J.; van Duin, A.; Mathews, J. P. Sulfur removal from petroleum coke during high-temperature pyrolysis. Analysis from TG-MS data and ReaxFF simulations. *J. Anal. Appl. Pyrolysis* **2018**, *132*, 134−142.
(37) Xiao, J.; Li, F.; Zhong, Q.; Huang, J.; Wang, B.; Zhang, Y. Effect of high-temperature pyrolysis on the structure and properties of coal and petroleum coke. *J. Anal. Appl. Pyrolysis* **2016**, *117*, 64−71.

https://doi.org/10.1021/acsomega.3c01446
ACS Omega 2023, 8, 18140−18150